AGU PUBLICATIONS

Water Resources Research

RESEARCH ARTICLE
10.1002/2014WR015607

Analysis of subsurface storage and streamflow generation in urban watersheds

Aditi S. Bhaskar[1,2] and Claire Welty[1]

[1]Department of Chemical, Biochemical and Environmental Engineering, Center for Urban Environmental Research and Education, University of Maryland, Baltimore County, Baltimore, Maryland, USA, [2]Now at U.S. Geological Survey, Eastern Geographic Science Center, Reston, Virginia, USA

Key Points:
- Rainfall depth and not watershed storage controls pre-event water proportion
- The most urban watershed has the largest streamflow sensitivity to storage
- Hillslope simulations show that the storage-streamflow relationship is hysteretic

Correspondence to:
A. S. Bhaskar,
abhaskar@usgs.gov

Citation:
Bhaskar, A. S., and C. Welty (2015), Analysis of subsurface storage and streamflow generation in urban watersheds, *Water Resour. Res.*, *51*, 1493–1513, doi:10.1002/2014WR015607.

Received 20 MAR 2014
Accepted 14 JAN 2015
Accepted article online 21 JAN 2015
Published online 13 MAR 2015

Abstract Subsurface storage as a regulator of streamflow was investigated as an explanation for the large proportion of pre-event water observed in urban streams during storm events. We used multiple lines of inquiry to explore the relationship between pre-event water proportion, subsurface storage, and streamflow under storm conditions. First, we used a three-dimensional model of integrated subsurface and surface flow and solute transport to simulate an idealized hillslope to perform model-based chemical hydrograph separation of stormflow. Second, we employed simple dynamical systems analysis to derive the relationship between subsurface storage and streamflow for three Baltimore, Maryland watersheds (3.8–14 km^2 in area) along an urban-to-rural gradient. Last, we applied chemical hydrograph separation to high-frequency specific conductance data in nested urban watersheds (~50% impervious surface cover) in Dead Run, Baltimore County, Maryland. Unlike the importance of antecedent subsurface storage observed in some systems, we found that rainfall depth and not subsurface storage was the primary control on pre-event water proportion in both field observations and hillslope numerical experiments. Field observations showed that antecedent stream base flow did not affect pre-event water proportion or streamflow values under storm conditions. Hillslope model results showed that the relationship between streamflow values under storm conditions and subsurface storage was clockwise hysteretic. The simple dynamical systems approach showed that stream base flow in the most urbanized of three watersheds exhibited the largest sensitivity to changes in storage. This work raises questions about the streamflow generation mechanisms by which pre-event water dominates urban storm hydrographs, and the shifts between mechanisms in rural and urban watersheds.

1. Introduction

Subsurface flow commonly contributes to streamflow over a range of flow conditions, including stormflow. Many studies of undeveloped areas have found that pre-event water, also termed old water or water that is present in the watershed before a precipitation event, dominates streamflow during storm events (here termed stormflow) [*Buttle*, 1994; *Genereux and Hooper*, 1999]. In his commentary about the future of chemical hydrograph separation, *Burns* [2002] asks, "What about catchments in which people live and work?" It is a common assumption that urban areas are one of the few places where infiltration-excess (Hortonian) overland flow is the principal stormflow generation process [*Freeze*, 1974; *Nolan and Hill*, 1990; *Buttle*, 1994; *Burns*, 2002; *Spence*, 2010], meaning that impervious surfaces generate stormflow and the subsurface contributes little. Yet significant pre-event water proportions of stormflow have been observed in urban watersheds [*Nolan and Hill*, 1990; *Buttle et al.*, 1995; *Gremillion et al.*, 2000; *Pellerin et al.*, 2008; *Meriano et al.*, 2011], exposing our lack of understanding about where and how stormflow is generated.

1.1. Stormflow Generation Mechanisms

Chemical storm hydrograph separation has been used as a method to distinguish between temporal origins of streamflow (pre-event and event water), but this is not equivalent to streamflow separation by source (groundwater, unsaturated flow, overland flow), or flow paths [*Sklash and Farvolden*, 1979]. For example, rainwater infiltrating into the subsurface and quickly discharging to streams may retain the chemical signature of event water although it traveled to the stream by a subsurface pathway. The converse, pre-event water appearing at the surface, can occur due to mixing between surface and subsurface water at saturated

patches. Nevertheless, some researchers refer to pre-event and event water as groundwater and surface water, respectively [*Buttle et al*., 1995]. Chemical hydrograph separation does not provide information on mechanisms of streamflow generation. It is still an open question in hydrology precisely how pre-event water, which is thought to largely be slow-moving subsurface flow, responds so quickly and significantly to precipitation events in moving from the subsurface to the stream. *Kirchner* [2003] called this the "rapid mobilization of old water" paradox.

A number of conceptualizations have been set forth on how stormflow is generated, with some hypotheses falling out of favor over time. The idea that stormflow is generated by variable source areas has been updated to recognize that areas contributing to overland flow are not necessarily contiguous, continuous, or centered on the stream network [*McDonnell*, 2003; *Spence*, 2010]. It is not clear, however, how the variable-source-area concept could lead to pre-event water dominating storm hydrographs. Subsurface flow resulting from a storm, also called subsurface stormflow, has been suggested by a number of researchers, including those utilizing chemical hydrograph separation [e.g., *Kienzler and Naef*, 2008], to be an important process. Some conceptualizations of how subsurface stormflow is activated are discussed below.

From detailed field measurements at the Panola research site in the Georgia Piedmont, *Tromp-van Meerveld and McDonnell* [2006] found that the dominant mechanism generating subsurface flow from storms was lateral flow at the soil-bedrock interface. They called this the "fill-and-spill" mechanism [*Spence and Woo*, 2003], because saturation connectivity and filling of bedrock topography is a necessary threshold before spilling, or connected subsurface flow leading to streamflow, can occur. Below a precipitation threshold, saturation at the soil-bedrock interface was patchy. Once this precipitation threshold was crossed, subsurface stormflow was generated because the bedrock topographic lows were filled and connected to the hillslope outflow and excess water spilled out. Yet, the subsurface stormflow measured at the Panola hillslope site was relatively small (maximum of 7 mm for a 60 mm storm), and not observed at a watershed scale to determine whether significant streamflow was produced through this subsurface flow generation mechanism.

Modeling studies of hydrologic response to precipitation inputs have been developed to investigate the sensitivity of subsurface stormflow generation to various hillslope factors. These studies have found that specific yield [*Weiler and McDonnell*, 2004], bedrock permeability [*James et al*., 2010], bedrock leakage [*Tromp-van Meerveld and Weiler*, 2008], catchment slope angle, and bedrock topography contributing area [*Hopp and McDonnell*, 2009] play a role in controlling subsurface hydrologic response to storms. These hillslope modeling studies have a number of limitations, however. None of them include overland flow, which is important to include in cases where this phenomenon may be relevant (for example, in urban areas). Few studies have performed numerical chemical hydrograph separation using a solute transport model [*Weiler and McDonnell*, 2004] possibly because in systems other than urban ones, stormflow is dominated by pre-event water.

Graham and McDonnell [2010] compared two streamflow-generation hypotheses using numerical experiments to implement a conceptual mathematical model. The bedrock-detention-storage hypothesis postulates that streamflow generation is controlled by bedrock permeability and subsurface storage volume. The prestorm moisture-deficit hypothesis states that streamflow generation is regulated by antecedent moisture and potential evapotranspiration. The results of numerical experiments showed that antecedent moisture controlled the threshold value of precipitation for the onset of subsurface stormflow generation. Above the precipitation threshold, bedrock permeability and subsurface storage volume determined the slope of the precipitation-streamflow relationship. This research made explicit the theorized connection between watershed storage and streamflow generation.

1.2. Subsurface Storage and Relationship to Streamflow

Subsurface storage is difficult to measure and has received little attention compared to measurement and analysis of streamflow and precipitation. Nevertheless, the relationship between streamflow and storage has long been sought [*Beven*, 2006]. Storage has also been proposed as a component of a catchment classification framework [*McDonnell and Woods*, 2004; *Wagener et al*., 2007; *McNamara et al*., 2011]. Furthermore, some researchers have suggested that storage may control streamflow and have called for a greater understanding of the storage dynamics of watersheds [*Spence*, 2010; *Sayama et al*., 2011]. Storage is critical to the emerging paradigm of streamflow generation as a set of "threshold-mediated, connectivity-controlled

processes" [*Spence*, 2010]. Threshold behavior in the relationship between precipitation and streamflow has been observed by researchers for diverse hydrogeologic and climatic settings [*Tromp-van Meerveld and McDonnell*, 2006; *McGuire and McDonnell*, 2010; *Graham and McDonnell*, 2010; *Sayama et al*., 2011; *Zehe and Sivapalan*, 2009]. The precipitation value at which this threshold occurs may be storage dependent [*Graham and McDonnell*, 2010], meaning that precipitation alone is not a predictor of streamflow. Threshold behavior has also been observed between storage (or antecedent moisture) and streamflow response [*Sidle et al*., 2000; *Spence*, 2007; *Detty and McGuire*, 2010; *Teuling et al*., 2010; *Oswald et al*., 2011].

Both precipitation-streamflow and storage-streamflow thresholds may be explained by precipitation first filling available storage reservoirs with little streamflow response. After a threshold in storage is reached, such as when bedrock topographic lows are filled, subsurface stormflow generation is activated and subsequent precipitation leads to large changes in hillslope or watershed outflow. This behavior was observed by *Sayama et al*. [2011] for storage and streamflow of 17 watersheds in the Pacific Northwest. Using water balance methods, they found that the watersheds had variable maximum storage volumes, ranging from 200 to 500 mm. The maximum watershed storage was most correlated with mean watershed topographic gradient, which they attributed to a larger hydrologically active bedrock zone.

Kirchner [2009] proposed a methodology to develop the relationship between storage and streamflow in which watersheds are treated as simple dynamical systems. During periods of low precipitation and evapotranspiration, changes in storage are assumed to be primarily related to streamflow. This approach assumes that streamflow is solely related to storage, and as *Kirchner* [2009] states, may not work for watersheds in which there is significant overland or bypassing flow. This methodology and modifications of the method have been applied to a number of areas characterized by low levels (0–27%) of urban cover [*Kirchner*, 2009; *Majone et al*., 2010; *Teuling et al*., 2010; *Krier et al*., 2012; *Xu et al*., 2012; *Ajami et al*., 2014]. The method has not been tested on data from urban watersheds, and therefore, the limits to the method are not known. It is not clear how urban development (e.g., impervious cover, compacted fill, pipes) may affect the relationship between storage and streamflow.

1.3. Chemical Hydrograph Separation Studies

Studies of chemical or isotopic storm hydrograph separation in urban watersheds have reported a wide range of pre-event water contributions (0–89%), sometimes within the same watershed. Tracers commonly used to perform hydrograph separations include specific conductance (primarily due to chloride content) and deuterium. *Buttle et al*. [1995] examined an Ontario catchment with 14% hydraulically connected impervious area, and found that 45–52% of stormflow due to snowmelt was pre-event water. *Sidle and Lee* [1999] used deuterium to separate hydrographs in a first-order stream near Cincinnati, Ohio, and found that 62–76% of the storm water was pre-event water. *Gremillion et al*. [2000] found that the pre-event water proportion of a developed watershed was 47%, as compared to 76% in the upstream, less developed, portion of the Florida stream. *Pellerin et al*. [2008] analyzed a Massachusetts basin with 25% impervious area, and found 22–82% of stormflow was pre-event water, and was related to antecedent streamflow over multiple storms. *Meriano et al*. [2011] studied a 75% urbanized watershed in Ontario and calculated that 23–30% of stormflow was pre-event water. *Nolan and Hill* [1990] determined that 57–89% of stormflow in an urban watershed in California was pre-event water, where 14% of the watershed area was delineated as limestone quarry, and 6% was designated as impervious surface cover. The authors suggested that the cause was in-channel (pre-event) water being displaced downstream soon after rainfall by additional event water from the channel upstream. This explanation does not appear to be generally applicable, however, because the time of elevated pre-event water observed in many storms is longer than the few minutes they calculated for the travel time of the in-stream flood wave. The mechanisms that led to highly variable pre-event water proportion (which at times exceeds half of stormflow) in urban watersheds are not yet known.

1.4. Purpose and Scope

Thresholds and connectivity of watershed storage have been suggested as physical characteristics controlling streamflow generation from subsurface sources [*Spence*, 2010; *Sayama et al*., 2011]. However, the controls on the relationship between storage and stormflow and the role of fill-and-spill storage thresholds in stormflow generation are not well understood, and there is virtually no information on this phenomenon for urban areas. The percentage of people living in cities globally was 30% in 1950, 54% in 2014, and is expected to grow to 66% in 2050 [United Nations, 2014]. Accompanying expansion of urban populations

are changes in land cover and land use, which in turn alter the hydrologic cycle [*Paul and Meyer*, 2001; *Rose and Peters*, 2001; *Walsh et al*., 2005; *Bhaskar and Welty*, 2012; *Kaushal and Belt*, 2012]. Managing water resources for these populations exposed to changes in land use, and climate is a key challenge for the field of hydrologic science [*Wagener et al*., 2010]. Meeting this challenge requires development of a robust, process-based understanding of the impact of urbanization on water fluxes, flow paths, and stores, an understanding we are currently lacking.

Here we focus on subsurface storage, with the assumption that subsurface storage comprises the greatest percentage of watershed storage in these landscapes. Surface depression storage has been explored as significant in controlling streamflow in other landscapes such as the Canadian prairie [*Ehsanzadeh et al*., 2012]. With their wide range of pre-event water responses, urban watersheds can be viewed as end-members in investigating controls on stormflow generation. Quantification of the subsurface contribution to flashy stormflow could contribute to improved management of urban streams [*Walsh et al*., 2005].

This work seeks to better quantify the controls on and relationship between pre-event water proportion, streamflow, and subsurface storage in urban areas. Specifically, we seek to answer the following questions:

1. What controls pre-event water proportion of stormflow in urbanizing areas?
2. What controls the relationship between subsurface storage and streamflow along an urban-to-rural gradient?
3. What is the relationship between pre-event water proportion of stormflow and subsurface storage in urban areas?

The controls investigated were percent impervious surface coverage and storm size (Questions 1 and 2) as well as the control of initial subsurface storage on pre-event water proportion (Question 3), and were evaluated using a combination of idealized numerical experiments and analysis of field data from the Baltimore, Maryland area.

2. Methods

We approached these research questions using a combination of three methods. First, we developed model of integrated subsurface and surface flow and solute transport of an idealized hillslope and conducted numerical experiments to explore changes in pre-event water proportion and the relationship between storage and streamflow (section 2.1). Second, we applied the simple dynamical systems approach [*Kirchner*, 2009] to hydrometric data from three watersheds along an urban-to-rural gradient in Baltimore County, MD to develop storage-streamflow relationships for these watersheds (section 2.2). Third, we carried out chemical hydrograph separation using high-frequency specific conductance data to determine pre-event and event contributions to stormflow for a set of six small, nested, urban watersheds in Baltimore County, MD (section 2.3).

2.1. Hillslope Numerical Experiments

With field observations, it is nearly impossible to alter watershed characteristics in order to observe the effects on a measurement of interest. Numerical modeling is well suited to address this limitation. Although mathematical models are simplified representations of reality, they allow watershed characteristics to be systematically varied in order to better understand the interactions and factors that control hydrologic behavior. This type of analysis can be viewed as conducting "virtual experiments" [*Weiler and McDonnell*, 2004; *Hopp and McDonnell*, 2009], where understanding of patterns and controls across watersheds, instead of cataloguing the functionality of an individual watershed, can be advanced [*McDonnell*, 2003].

We used HydroGeoSphere as a tool to evaluate the controls on pre-event water proportion of an idealized watershed. HydroGeoSphere uses a control volume finite element scheme to solve coupled three-dimensional surface-subsurface fluid flow and solute transport equations [*Therrien et al*., 2010], and has been used to carry out model-based chemical hydrograph separation [*Jones et al*., 2006; *Park et al*., 2011]. We developed an implementation of the model to represent an idealized hillslope in order to examine the effect of changes to hillslope properties. We focused on storm simulations using small, adaptive time steps (between 1×10^{-6} and 100 s). The simulations were generally 200,000 s (2.3 days) long, except for the simulation with impervious surface cover (described in section 2.1.1), which was run for double this amount of

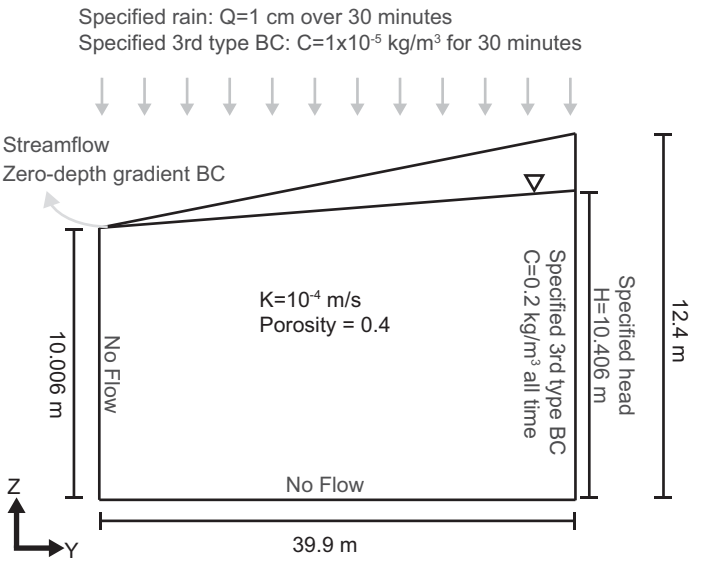

Figure 1. Schematic of hillslope model domain and setup. Not to scale. The model domain is three-dimensional, but only a two-dimensional Y-Z slice is shown.

time because of the slow return to solute concentration conditions at base flow. The modeled pre-event water was assigned a conservative solute concentration distinct from that in event (rain) water, and the solute concentration in the modeled stormflow was used to partition streamflow between pre-event and event water. We used chloride as the conservative solute because of its distinct signature in groundwater in urban areas where there is accumulated chloride from road salt application [*Gelhar and Wilson*, 1974] such that the chloride concentration in groundwater greatly exceeds the chloride concentration in rain.

The idealized domain was designated as 39.9 m in the horizontal direction perpendicular to the stream (*y* axis), 0.9 m parallel to the stream (*x* axis), and ranged from 10.006 to 12.4 m in thickness (*z* axis) (Figure 1). We assumed a value of 1 cm for isotropic local dispersivity in all three directions. In order to minimize numerical dispersion and spurious oscillations, we kept the grid Peclet number less than 10 by setting the discretization less than 0.1 m in all dimensions. Specifically, *dx* was 0.09975 m, *dy* was 0.09 m, and *dz* varied between 0.08 and 0.1 m along the *y* direction. The model consisted of 124 layers regardless of total model thickness. Therefore, the number of model grid cells was 400 × 10 × 124, or 496,000. The land surface was assigned a constant slope of 0.06. The material property values used in the base-case model (no impervious surfaces; rainfall depth of 1 cm) are listed in Table 1. The "dual nodes" option in HydroGeoSphere was chosen for coupling subsurface with surface flow, and tables were generated to approximate unsaturated zone functions.

The surface flow boundary condition at the line of stream cells (along the *x* direction) was a zero-depth hydraulic gradient boundary with the bed-slope equal to the land surface slope of 0.06. The boundary condition at the up-gradient face of the domain was specified as a hydraulic head value of 10.406 m. The transport boundary condition at the up-gradient face was specified as a third-type condition with a chloride concentration of 0.2 kg/m^3. The top of the model domain, which allowed for overland flow, was assigned a specified rainfall flux boundary condition of 5.555×10^{-6} m/s for 30 min as well as a third-type transport boundary condition with a chloride concentration of 1×10^{-5} kg/m^3 during the rain period (30 min from 10,000 to 11,800 s).

Table 1. Hydrogeologic Properties and Parameters Used in Hillslope Model[a]

Property	Value
Total porosity	0.4
Hydraulic conductivity	1×10^{-4} m/s
Specific storage	1×10^{-6} m^{-1}
Tortuosity	0.05
van Genuchten parameter α	2 m^{-1}
van Genuchten parameter β	2
Residual saturation	0.1
Unsaturated zone minimum pressure head	−50 m
Dispersivity	0.01 m

[a]Values shown are the base case model values, some of which are modified in numerical experiments (Table 3).

To initialize the model, we first ran a steady state simulation with an initially linear water table hydraulic gradient defined by hydraulic head values ranging from 10.006 m at the stream cells to 10.406 m at the up-gradient face of the domain. The hydraulic head output from the steady state simulation was used as the initial condition for the transport model, which was transient and was run for 200,000 s (2.3 days). In the transient transport simulation, precipitation was introduced as well as a groundwater background chloride concentration of 0.2 kg/m^3. The head and concentration output from this transient simulation were used as initial conditions for the numerical experiments described in

sections 2.1.1 and 2.1.2. The material properties, model domain, and boundary conditions used in the base case of the numerical experiments are summarized in Figure 1.

2.1.1. Numerical Experiments of Controls on Pre-event Water Proportion

Two parameters were varied to investigate the sensitivity of pre-event water proportion: watershed imperviousness and storm size (rainfall depth). Watershed imperviousness was selected as a parameter of interest because of the potential importance of infiltration-excess overland flow for conditions with particularly high-precipitation intensities or percent impervious surface area. Impervious surfaces were represented by lowering saturated hydraulic conductivity to a value of 1×10^{-7} m/s [*Wiles and Sharp*, 2008], and lowering porosity to a value of 0.05 [*Liu and Guo*, 2003] compared to the base case. Watershed percent impervious area was set at 0% in the base-case model, and 100% in the impervious surface cover model. At 100% impervious surface cover, low hydraulic conductivity and porosity values representing imperviousness were specified for the entire hillslope.

Storm size was found to influence the pre-event water proportion in an analysis of Dead Run specific conductance records; this is why we chose to vary storm size in the hillslope numerical experiments. Storm size was altered by changing rainfall depth from the base-case value of 1 cm to values of 0.25, 0.75, 1.25, and 2.5 cm, while duration of the rain event was constant at 30 min. Other temporally varying parameters, such as antecedent moisture or time between storms, were not evaluated because the effects of these were represented by initial storage conditions of the watershed (section 2.1.2).

2.1.2. Numerical Experiments of Controls on Storage-Streamflow Relationship

Hillslope storage before the rain event was varied by changing the position of the water table at the beginning of the transport simulation (starting with output from the steady state flow initialization). Initial water table elevation at top of the hillslope was varied between 10.406 m (base case) and 11.2036 m. Subsurface storage was determined by postprocessing simulation results to calculate the volume of water present in every grid cell within the domain. A macro developed in Tecplot 360 was used to process exported HydroGeoSphere files as follows:

$$\begin{aligned} Subsurface\ \ Storage\,[L^3] = Saturation[-] \times Porosity[-] \times dx[L] \times dy[L] \times dz[L] + \\ Saturation[-] \times Pressure\ \ Head[L] \times Specific\ \ Storage[L^{-1}] \times dx[L] \times dy[L] \times dz[L] \end{aligned} \tag{1}$$

The resulting gridded subsurface storage was then summed over the entire subsurface to calculate total subsurface storage in the domain.

Streamflow was also exported as a function of time. The effects of varying initial water table position, imperviousness, and storm size on the relationship between storage and streamflow were evaluated. The pre-event water proportion was calculated by using a binary mixing model applied to model output under various subsurface storage conditions. The relationship between pre-event water proportion and storage was thus developed for the idealized hillslope. Table 3 shows the parameter values for all hillslope numerical experiments used to address Questions 1–3 (section 1.4).

2.2. Simple Dynamical Systems to Develop Storage-Streamflow Relationship

We used the simple dynamical systems approach by *Kirchner* [2009] to develop storage-streamflow relationships for three Baltimore watersheds characterized by a range of urban development. The method uses a water balance formulation where water enters storage (S) from precipitation (P) and exits storage through evapotranspiration (ET) and streamflow (Q; also termed discharge). This method assumes that streamflow is solely a function of storage:

$$\frac{dS}{dt} = P - ET - Q \tag{2a}$$

where

$$Q = f(S) \tag{2b}$$

The streamflow sensitivity function $g(Q)$ used by *Kirchner* [2009] is defined by the change in streamflow per change in storage. We used streamflow records from rainless nights and assumed that precipitation and

evapotranspiration were small relative to streamflow during these time periods. The streamflow sensitivity function was empirically estimated using the streamflow record from [*Kirchner*, 2009]

$$g(Q)=\frac{dQ}{dS}=\frac{dQ/dt}{dS/dt}=\frac{dQ/dt}{P-ET-Q}\approx\left.\frac{-dQ/dt}{Q}\right|_{P\ll Q,ET\ll Q}. \tag{3}$$

The relationship between storage and streamflow was found by analytical integration of the sensitivity function:

$$S=\int\frac{dQ}{g(Q)} \tag{4a}$$

$$S(a)=\int_1^a\frac{1}{g(Q)}dQ \tag{4b}$$

We applied this method to three similarly sized watersheds along an urban-to-rural gradient in the Baltimore Ecosystem Study Long-Term Ecological Research (BES LTER) study area (Figure 2 and Table 2) that are instrumented with USGS stream gages at their outlets. These watersheds lie within the Piedmont physiographic province and are underlain by fractured crystalline bedrock. Dead Run (Dead Run at Franklintown, http://waterdata.usgs.gov/md/nwis/uv/?01589330) is a 14.1 km^2 suburban watershed characterized by 45% impervious surface area and a mixture of residential, commercial, and transportation land use, with two major interstate highways bisecting its drainage area. Delight (Gwynns Falls Near Delight http://waterdata.usgs.gov/usa/nwis/uv?01589197) is a 10.6 km^2 watershed composed of 19% impervious surface area, with largely residential suburban land use. Baisman Run (Baisman Run at Broadmoor, http://waterdata.usgs.gov/usa/nwis/uv?01583580) is 3.8 km^2 in area, with only 2% impervious land cover, and is largely forested, with low-density residential land use.

We used USGS streamflow records from 2002 to 2008 at these stream gages, and standardized the time increments for hourly analysis. Streamflow was converted to units of mm/h by scaling by watershed area (Table 2). The time period spanned extremes in dry (820 mm rain in 2002) and wet (1630 mm rain in 2003) years. Because of gaps in precipitation data, we used the average of two data sets: bias-corrected Hydro-NEXRAD and Stage IV radar-rainfall fields [*Smith et al*., 2012; M. L. Baeck and J. Smith, personal communication, 2012]. Any remaining time periods for which streamflow was rising but precipitation records were missing were excluded from analysis. Total solar irradiance was estimated with a LI-COR (Lincoln, NB) silicon pyranometer at the BES LTER meteorological station at McDonogh (Figure 2). Rainless time periods were defined as those with no precipitation for the previous 6 h and the subsequent 2 h. Night times were isolated by selecting times when the average solar irradiance over a 3 h time window was <1 W/m^2. These two criteria were combined such that rainless night times could be selected for analysis, based on *Kirchner* [2009]. The binning and fitting procedure used was similar to that in *Kirchner* [2009], in which bins contained at least 1% of all $-dQ/dt$ values and where the standard error of the values in each bin was less than $^1/_2$ of the mean of the $-dQ/dt$ bin values. A piecewise linear fit of $\ln(Q)$ versus $\ln(-dQ/dt)$ was used in logarithmic space in order to provide a reasonable fit to the data. The data from the BES LTER meteorological station at McDonogh were also used to calculate potential evapotranspiration using the Penman-Monteith formulation [*Allen et al*., 1998; G. Heisler, personal communication, 2012].

We evaluated the derived storage-streamflow relationships across the three Baltimore watersheds described above that are characterized by varying percentages of impervious surface coverage. We also compared the relationships for Baltimore, MD with those for the Severn and Wye Rivers in Wales, which are undeveloped watersheds of similar size and have been evaluated by *Kirchner* [2009].

2.3. Chemical Hydrograph Separation

YSI 600-LS conductivity/temperature sondes were deployed at USGS stream gaging stations at Dead Run Franklintown and its subwatersheds (Figure 2) [*VerHoef et al*., 2011; *VerHoef*, 2012], with specific conductance data collected every 30 min beginning in October 2010. In this region, stream base flow has a specific conductance signal 1–2 orders of magnitude greater than precipitation, owing to the accumulated road salt in the groundwater that is the source of streamflow. During rain events, the specific conductance of streamflow is greatly diluted by rainfall. The disparate specific conductance signal in stream base flow compared

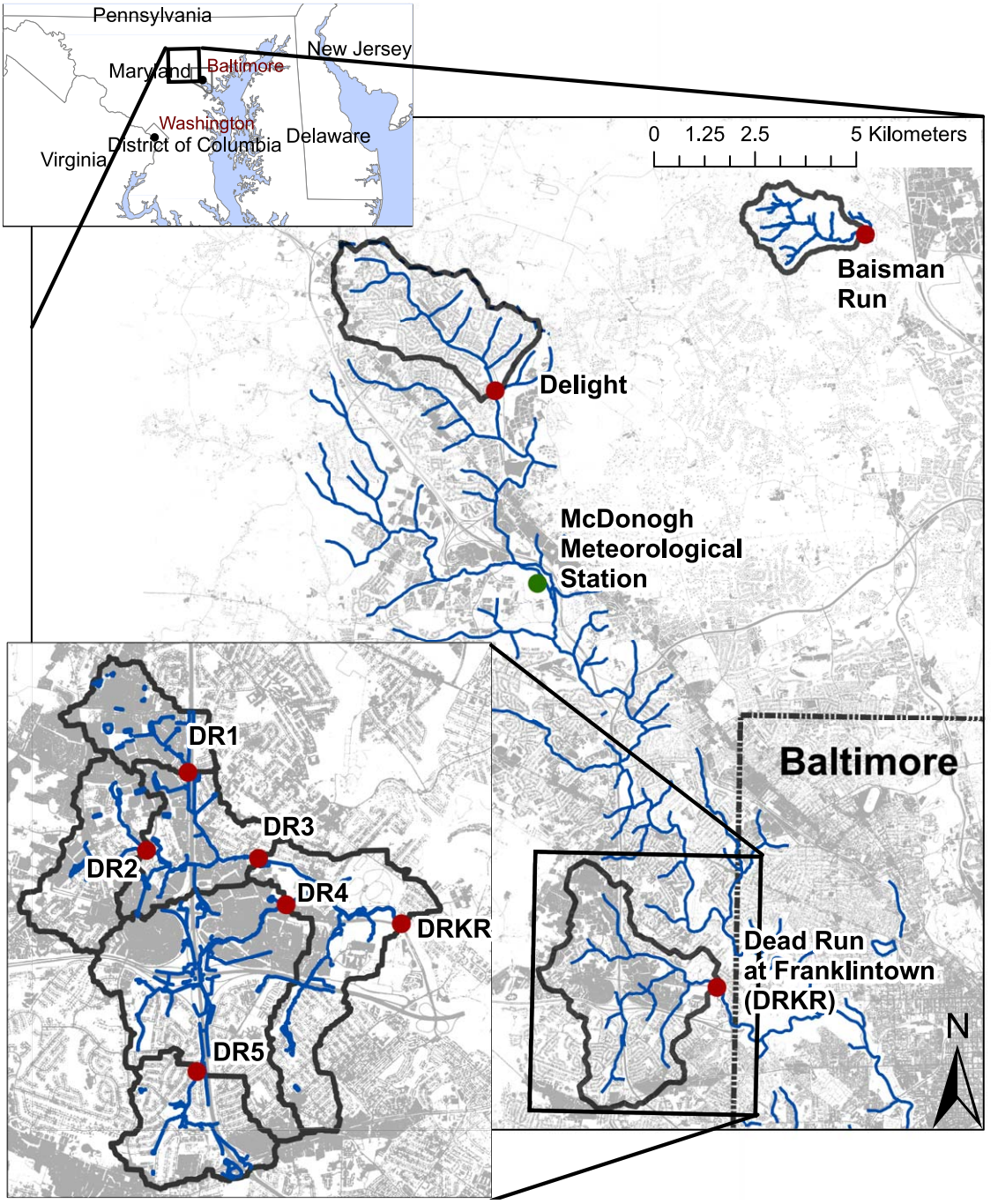

Figure 2. Map of watersheds used for simple dynamical systems analysis (Baisman Run, Delight, and Dead Run at Franklintown), and an inset showing subwatersheds of Dead Run used for the chemical hydrograph separation study (DRKR, DR1, DR2, DR3, DR4, and DR5). Red dots indicate USGS stream gages, gray scale indicates impervious surface cover, and blue lines represent hydrography (both daylighted and buried streams).

to rainfall and the colocation of the specific conductance and discharge measurements allows chemical storm hydrograph separation to be carried out.

Chemical hydrograph separation was computed using a simple two-component model [*Kendall and McDonnell*, 1999]. Pre-event streamflow (discharge) was taken as the streamflow value occurring immediately before the rising limb of the stormflow hydrograph. The return to this pre-event streamflow value was used to define the end of the stormflow hydrograph. The pre-event solute concentration was taken as the value of specific conductance at the time of the defined pre-event streamflow (ranging from 0.6 to 1.7 mS/cm). Event

Table 2. Characteristics of Watersheds Used for Chemical Hydrograph Separation and Simple Dynamical Systems Analysis

Watershed	USGS Site Number	Drainage Area (km^2)	Percent Impervious Surface Cover
Baisman Run	1583580	3.8	2.3
Delight	1589197	11	18.6
DR Franklintown (DRKR)	1589330	14	45.0
DR1	1589317	1.3	51.1
DR2	1589316	1.9	44.7
DR3	1589320	5.0	48.2
DR4	1589315	6.2	49.8
DR5	1589312	1.5	44.9

concentration, or the specific conductance of precipitation, was based on data from the Beltsville, MD National Atmospheric Deposition Program (NADP) station and was taken to be an average value of 0.025 mS/cm. Using this information along with recorded concentration and streamflow during the rain event, pre-event water proportion was calculated using:

$$\frac{Q_o}{Q_t} = \frac{C_n - C_t}{C_n - C_o} \tag{5}$$

where Q is streamflow (discharge), C is tracer concentration (specific conductance in our case), and the subscripts o, n, and t indicate old (pre-event) water, new (event) water, and total stream water, respectively. As the event water specific conductance was about 2 orders of magnitude smaller than pre-event water specific conductance, variations in event water specific conductance had little effect on resulting pre-event water proportion. Specific conductance (mS/cm) is linearly correlated to chloride concentration (mg/L) in these watersheds with an R^2 value of 1.00.

Dead Run chemical hydrograph separation results were compared to storage conditions during the time at which pre-event water proportion was calculated. Since watershed total storage conditions cannot be directly measured in the field, pre-event base flow (streamflow recorded just prior to the storm event) was used as a proxy for subsurface storage, based on the assumption (e.g., used in the simple dynamical systems analysis) that storage and streamflow have a one-to-one relationship.

3. Results

3.1. Controls on Pre-event Water Proportion

The simulated idealized model domain is shown to scale with hydraulic head (m) contours (Figure 3). The modeled storm event led to an increase in hydraulic head at the land surface, perturbing the prestorm hydraulic gradient defined by the boundary conditions. Simulations were run for 200,000 s or more, at which point streamflow, subsurface storage, and chloride were all back to base flow conditions. Total streamflow, calculated pre-event water, and calculated storage over time for the simulation runs listed in Table 3 are presented in Figure 4. Figure 4 focuses on the beginning of the simulation, on the time period bracketing the rain event. For the base-case model, streamflow reacted as expected, with streamflow slightly decreasing before the storm event, rising during the storm event, falling quickly after the rain stopped to near-base flow levels, and then receding more gradually to reach the base flow value occurring before the rain event (Figure 4a). The pre-event water proportion (Figure 4b) was calculated using equation (5). The computed pre-event water proportion for the entire simulation period is given in Table 3. The

Table 3. Parameter Values for Hillslope Numerical Experiments, as Well as Results for Pre-event Water Proportion of Storm Total for Each Case

Simulation	Hydraulic Conductivity (m/s)	Total Porosity	Rainfall Depth (cm over 30 min)	Initial Water Table Height (m) at Up-Gradient Face (y = 39.9 m)	Water Table Slope (m/m)	Calculated Pre-event Water Proportion (Over Entire Simulation)
Base case	10^{-4}	0.4	1.0	10.406	0.01	0.89
Impervious	10^{-7}	0.05	1.0	10.406	0.01	0.14
Largest storm	10^{-4}	0.4	2.5	10.406	0.01	0.74
Larger storm	10^{-4}	0.4	1.25	10.406	0.01	0.86
Smaller storm	10^{-4}	0.4	0.75	10.406	0.01	0.93
Smallest storm	10^{-4}	0.4	0.25	10.406	0.01	0.98
Initially wetter	10^{-4}	0.4	1.0	10.9045	0.023	0.90
Initially wettest	10^{-4}	0.4	1.0	11.2036	0.03	0.90

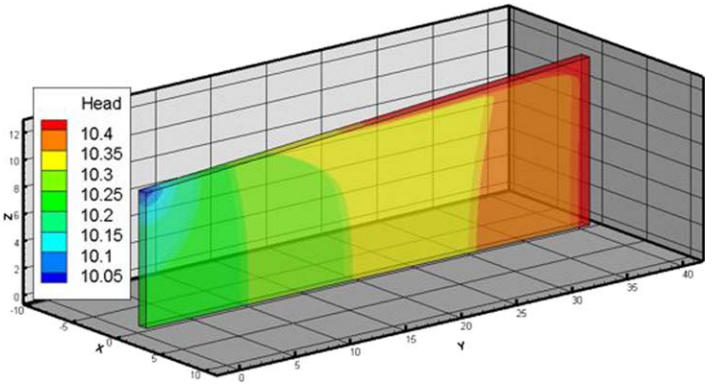

Figure 3. Model domain to scale of hillslope for base-case parameters. Colors indicate contours of head (m) at 14,000 s (37 min after the rain event ends).

chloride concentration, and therefore the pre-event water proportion (Figure 4b), had a drop that was longer in duration but of a similar shape as the streamflow response (Figure 4a).

For the impervious surface model, the streamflow response was much greater in magnitude and the pre-event water proportion was lower than the base case. The pre-event water proportion and subsurface storage took much longer to return to background levels in the impervious surface model because of the combination of low hydraulic conductivity slowing subsurface flow and lower porosity leading to less connected subsurface flow. The responses of the cases with changes in rainfall depth behaved as expected. The largest storm was characterized by the highest streamflow peak and a lower pre-event water proportion, whereas storms having rainfall depths smaller than the base case showed the opposite behavior. The cases specified with

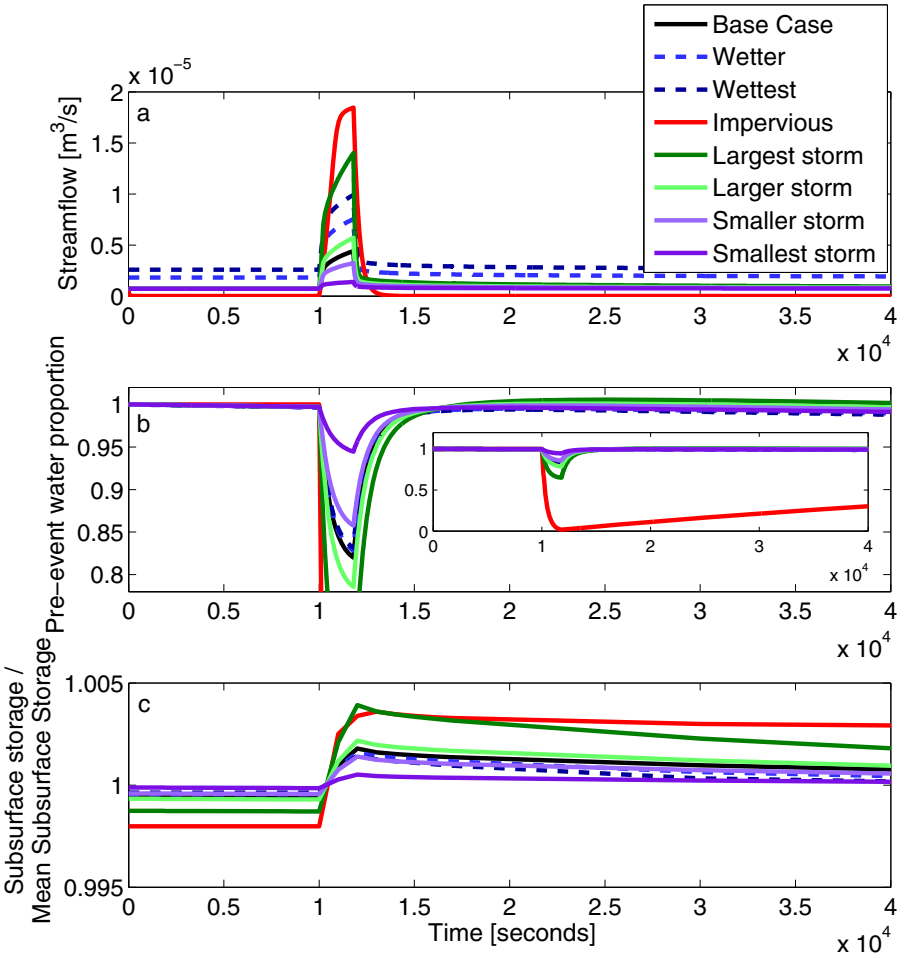

Figure 4. (a) Streamflow as a function of time from hillslope model simulations listed in Table 2. (b) Pre-event water proportion (equation (5)) for model simulations. Inset shows increased *y* axis range of pre-event water proportion. (c) Subsurface storage calculated by equation (1). Subsurface storage for each model is divided by its mean subsurface storage.

Table 4. Dead Run Subwatershed Chemical Hydrograph Separation for Storm Events

Station	Storm Start Date (MM/DD/YY)	Rainfall Depth (cm)	Rainfall Duration (h)	Time Since Last Rain (days)	Base Flow (cfs) Before Storm	Q_t (cm)	Fraction Pre-event Water (Q_o/Q_t)	Min Q_o/Q_t at Peak Storm Flow
DRKR	08/31/14	0.15	4.63	7.98	1.7	0.31	0.50	0.83
DRKR	11/07/13	0.18	1.28	2.85	1.2	0.10	0.94	0.87
DRKR	05/12/14	0.53	0.43	1.84	3.2	0.27	0.67	0.66
DRKR	10/19/10	0.97	6.27	3.60	1.4	0.46	0.46	0.2
DRKR	06/25/14	1.02	0.375	6.21	2	0.76	0.38	0.21
DRKR	10/14/10	2.1	6.78	6.90	1.4	0.87	0.22	0.07
DRKR	11/30/10	2.15	27	4.99	1.3	1.26	0.23	0.09
DRKR	11/03/10	2.82	17.3	7.40	1.1	1.51	0.22	0.05
DRKR	05/16/14	4.6	10.5	3.26	3.5	3.58	0.29	0.18
DRKR	05/11/13	4.78	49.8	0.81	2.2	3.29	0.23	0.09
DRKR	11/26/13	5.03	31.9	8.28	0.94	2.74	0.27	0.12
DRKR	04/28/14	11.23	46.1	2.76	2.9	14.20	0.23	0.12
DR5	05/12/14	0.53	0.4	1.84	0.61	0.45	0.56	0.44
DR5	05/07/14	0.64	1.7	1.10	0.69	0.42	0.73	0.81
DR5	04/19/11	0.65	5.8	2.44	0.24	0.34	0.63	0.33
DR5	06/25/14	1.02	0.375	6.21	0.69	0.33	0.68	0.69
DR5	04/08/11	1.21	15	2.70	0.22	0.47	0.47	0.23
DR5	04/25/14	1.21	6.62	2.82	0.57	0.49	0.58	0.33
DR5	11/30/10	2.15	27	4.99	0.22	0.94	0.36	0.2
DR5	04/16/11	2.9	15.2	2.80	0.22	1.38	0.27	0.15
DR5	08/21/11	3.62	8.7	2.20	0.3	1.43	0.24	0.04
DR5	05/16/14	4.6	10.5	3.26	0.57	2.37	0.29	0.12
DR5	05/11/13	4.78	49.8	0.81	0.43	1.65	0.28	0.1
DR5	11/26/13	5.03	31.9	8.28	0.37	2.61	0.34	0.08
DR5	04/28/14	11.23	46.1	2.76	0.57	11.13	0.23	0.07
DR4	08/31/14	0.15	4.6	7.98	0.92	0.18	0.40	0.37
DR4	04/22/14	0.44	7.2	3.97	0.89	0.15	0.78	0.95
DR4	05/12/14	0.53	0.4	1.84	0.76	0.26	0.55	0.42
DR4	05/07/14	0.64	1.7	1.10	1.03	0.20	0.65	0.65
DR4	05/10/14	0.81	8.8	2.99	0.89	0.22	0.65	0.53
DR4	04/25/14	1.21	6.6	2.82	0.76	0.45	0.42	0.36
DR4	11/30/10	2.15	27	4.99	0.46	0.98	0.23	0.13
DR4	08/21/11	3.62	8.7	2.20	0.39	0.99	0.14	0.05
DR4	05/16/14	4.6	10.5	3.26	0.89	2.47	0.23	0.15
DR4	05/11/13	4.78	49.8	0.81	0.65	2.53	0.19	0.08
DR4	11/26/13	5.03	31.9	8.28	0.46	2.11	0.37	0.07
DR4	04/28/14	11.23	46.1	2.76	0.76	12.10	0.17	0.06
DR3	08/31/14	0.15	4.6	7.98	0.67	0.41	0.36	0.21
DR3	04/19/11	0.65	5.8	2.40	1	0.32	0.56	0.28
DR3	04/08/11	1.21	15	2.70	0.6	0.53	0.49	0.26
DR3	04/25/14	1.21	6.62	2.82	2.9	0.71	0.55	0.45
DR3	11/30/10	2.15	27	4.99	1.4	1.10	0.17	0.08
DR3	04/16/11	2.9	15.2	2.80	0.73	1.80	0.26	0.14
DR3	08/21/11	3.62	8.7	2.20	0.5	0.70	0.17	0.08
DR3	05/11/13	4.78	49.8	0.81	0.3	2.01	0.19	0.08
DR3	11/26/13	5.03	31.9	8.28	0.19	1.93	0.15	0.06
DR3	04/28/14	11.23	46.1	2.76	2.9	15.90	0.18	0.09
DR2	08/31/14	0.15	4.6	7.98	0.27	0.38	0.38	0.19
DR2	11/07/13	0.18	1.28	2.85	0.05	0.06	0.76	0.54
DR2	06/25/14	1.02	0.38	6.21	0.61	0.39	0.42	0.23
DR2	04/25/14	1.21	6.62	2.82	0.3	0.40	0.60	0.3
DR2	04/16/11	2.9	15.2	2.80	0.23	1.52	0.37	0.1
DR2	08/21/11	3.62	8.7	2.20	0.06	0.48	0.16	0.07
DR2	05/16/14	4.6	10.5	3.26	0.61	2.89	0.34	0.26
DR2	05/11/13	4.78	49.8	0.81	0.1	2.79	0.16	0.08
DR2	11/26/13	5.03	31.9	8.28	0.1	2.35	0.15	0.05
DR2	04/28/14	11.23	46.1	2.76	0.24	13.35	0.26	0.24
DR1	11/07/13	0.18	1.28	2.85	0.18	0.12	0.85	0.67
DR1	04/08/11	1.21	15	2.70	0.39	0.74	0.51	0.23
DR1	11/30/10	2.15	27	4.99	0.21	1.30	0.25	0.12
DR1	04/16/11	2.9	15.2	2.80	0.44	2.33	0.28	0.13
DR1	08/21/11	3.62	8.7	2.20	0.12	0.79	0.17	0.05
DR1	05/11/13	4.78	49.8	0.81	0.24	2.08	0.30	0.08
DR1	11/26/13	5.03	31.9	8.28	0.18	2.51	0.21	0.12

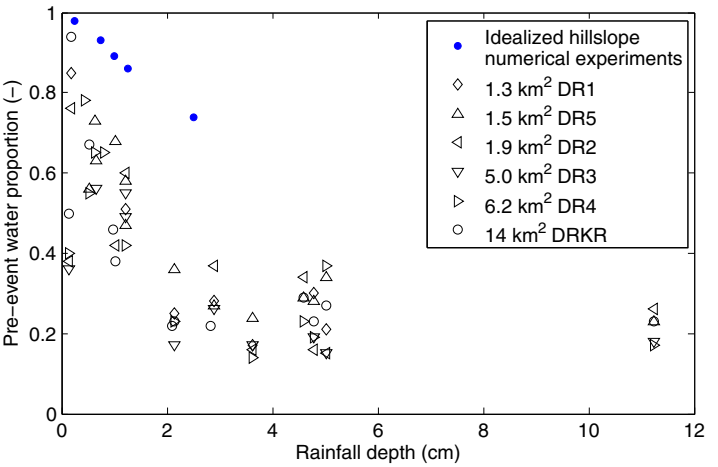

Figure 5. Pre-event water proportion as a function of rainfall depth for Dead Run and its subwatersheds. Black symbols indicate pre-event water proportion for storms of varying sizes (Table 4) using chemical hydrograph separation from Dead Run subwatersheds (Table 2). Blue circles indicate results from hillslope numerical experiments: the base case (1 cm rainfall) and the four cases of varying storm sizes (0.25, 0.75, 1.25, and 2.5 cm rainfall depths) and the associated pre-event water proportions (Table 3). Note these are not simulations of Dead Run but of an idealized hillslope, shown here only for comparison.

wetter initial conditions generated greater streamflow than the base case, but similar pre-event water responses compared to the base case.

We also used streamflow and specific conductance data collected in six nested watersheds in Baltimore, MD to analyze controls on pre-event water proportion. Sixty-four storm chemographs from Dead Run subwatersheds were analyzed by chemical hydrograph separation (Table 4 and Figure 5). Storms with smaller rainfall depths in the same watershed were found to be composed of a greater proportion of pre-event water. Other variables explored, such as days since prior rainfall, pre-event streamflow (base flow), and drainage size were not found to have a clear relationship with pre-event water proportion (Table 4). There was a close relationship between pre-event water proportion over the entire storm and the minimum pre-event water proportion occurring at peak streamflow.

3.2. Controls on Storage-Streamflow Relationship

Subsurface storage in the idealized model domain as a function of time was calculated from the numerical experiments (Figure 4c). Subsurface storage reached its prestorm value after approximately 150,000 s in the base-case model (it took more than double this time for the impervious surface simulation), but the entire simulation period is not shown so that the storm period can be illustrated more clearly. The relationship between streamflow (total and pre-event water) and subsurface storage for the base-case model is presented in Figure 6. This plot shows that the subsurface storage continued to increase slightly after the precipitation stopped and streamflow started to recede, with a hysteretic relationship between storage and streamflow as well as between storage and pre-event water. For the same subsurface storage value, the rising limb of the stormflow hydrograph had higher value than the falling limb. The pre-event water did not reach the same peak value as the total streamflow, but had a shape similar to total streamflow. Hydraulic head at the land surface before, during, and after the storm event for the base case is shown in Figure 7. Hydraulic head increases a function of distance from the stream, but the slope of this relationship varies with time. Water table mounding and dissipation near the stream is apparent.

The results from the simple dynamical systems analysis are shown in Figure 8. This figure displays plots of the natural logarithm of hourly change in streamflow as a function of the natural logarithm of streamflow for each of the three study watersheds described in section 2.2, along with bin means, and fits to these bins. The piecewise linear fits to the bins shown are given as:

$$\text{Dead Run}: \ln\left(\frac{-dQ}{dt}\right)=\begin{cases} 2.37\ \ln(Q)+1.93 & \text{if } \ln(Q) < -3.70 \\ 1.66\ \ln(Q)-0.71 & \text{if } -3.70 \le \ln(Q) < -2.02 \\ 1.22\ \ln(Q)-1.61 & \text{if } \ln(Q) \le -2.02 \end{cases} \quad (6a)$$

$$\text{Delight}: \ln\left(\frac{-dQ}{dt}\right)=\begin{cases} 2.03\ \ln(Q)-1.61 & \text{if } \ln(Q) < -3.20 \\ 3.86\ \ln(Q)+4.25 & \text{if } -3.20 \le \ln(Q) < -2.44 \\ 1.61\ \ln(Q)-1.25 & \text{if } \ln(Q) \le -2.44 \end{cases} \quad (6b)$$

$$\text{Baisman}: \ln\left(\frac{-dQ}{dt}\right) = \begin{cases} 4.05\ \ln(Q) + 2.37 & \text{if } \ln(Q) < -2.20 \\ 6.80\ \ln(Q) + 8.42 & \text{if } -2.20 \le \ln(Q) < -1.96 \\ 1.83\ \ln(Q) - 1.29 & \text{if } \ln(Q) \le -1.96 \end{cases} \quad (6c)$$

The linear plots of ln(Q) versus ln(−dQ/dt) in Figure 8 show that Dead Run had the highest streamflow values, whereas the streamflow values for Baisman Run were constrained to a narrow portion of the plot, and were always less than 0.5 mm/h. In logarithmic space, the resolution of the data becomes evident at Baisman Run, as each 0.3048 cm (0.01 ft) increment of stream stage represents a greater portion of the overall value of stream stage as stage decreases. The resolution of the streamflow data, and multiples of this resolution, formed horizontal lines where finer changes of streamflow over an hour are irresolvable. This is somewhat apparent for Delight and Dead Run at low flows as well.

The time period of study included a drought year (2002) when Baisman Run went dry. This was not plotted on a logarithmic scale, but was included in the bins and the fits to the bins. Baisman Run had a strong streamflow diurnal cycle, which was particularly evident during dry summers. This led to some rainless night times that had increases in streamflow due to recovery from evapotranspiration pumping during the day. Therefore, there were bin means for which $-dQ/dt$ was negative for Baisman, which is why the bin fits appear to not match the logarithmic data as well as the linear data. At very low flows, $-dQ/dt$ was constrained to a narrow range around 0, and increased to positive values. These are the four outliers that can be seen in the logarithmic plot for Baisman Run that were not considered in the fit.

The fits of Figure 8 (transformed to streamflow sensitivity by dividing $-dQ/dt$ by Q), as well as the streamflow sensitivity functions reported in *Kirchner* [2009] are displayed in Figure 9. For most of the range of streamflow values shown in the logarithmic plot, Dead Run, the most urban watershed, had the highest streamflow sensitivity, followed by Delight, the next most urban watershed as defined by percent impervious area. A high streamflow sensitivity at a given streamflow value means that the watershed has a high rate of change of streamflow for a given change in storage. The streamflow sensitivity of Baisman Run crossed above the streamflow sensitivity of the other watersheds at the highest streamflow values, where the sensitivity has been extrapolated beyond observed streamflow data. The method used to derive this function considered only data on the falling limb during rainless night times, meaning that the streamflow sensitivity function is calculated over a streamflow range that is limited, compared to the entire range of values present in the streamflow record.

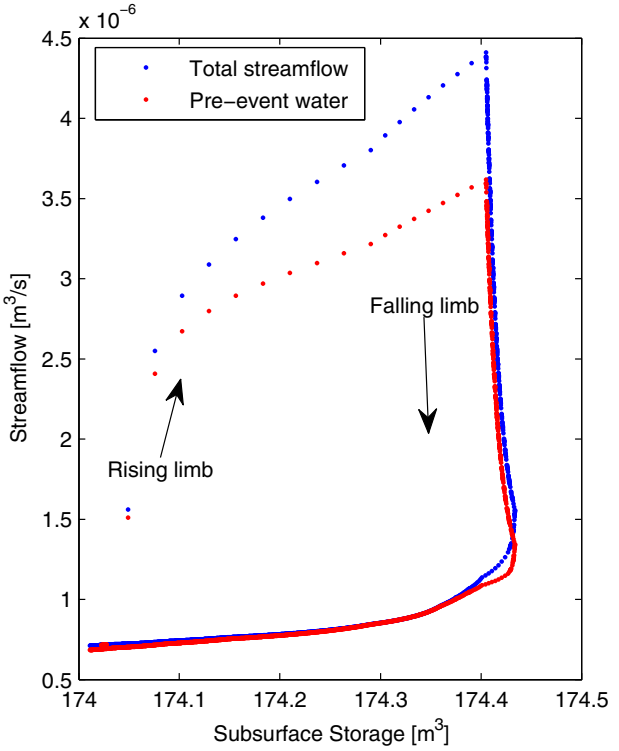

Figure 6. Total streamflow and pre-event streamflow as a function of subsurface storage, using base-case parameters in hillslope numerical experiments. Arrows indicate time, where "rising limb" and "falling limb" correspond to the associated components of total storm and pre-event storm hydrographs.

Integration of the streamflow sensitivity function was used to find the relationship between streamflow and storage for each watershed (Figure 10). This was derived through integration to an additive constant (constant of integration), and therefore the relative x position of these watersheds is arbitrary, but the relative slopes can be compared. Based on the higher streamflow sensitivity functions (Figure 9), all three study watersheds were characterized by steeper storage-streamflow relationships compared to those presented in the literature for which this analysis has been carried out previously.

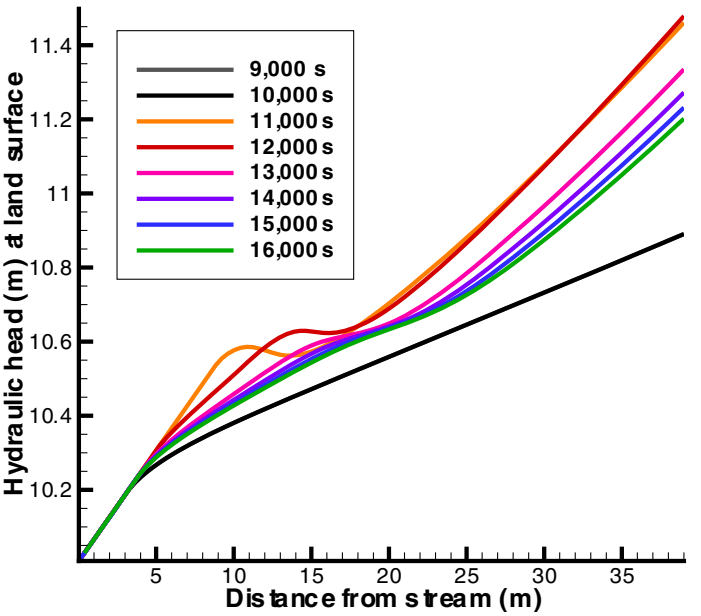

Figure 7. Hydraulic head (m) at the land surface as a function of distance from stream (m), shown for multiple time points for the base-case hillslope simulation. Before the storm, the hydraulic head was relatively constant, so the curve for 9000 s is directly underneath the curve for 10,000 s.

3.3. Relationship Between Storage and Pre-event Water Proportion

For Dead Run subwatersheds, there was little relationship between pre-event water proportion determined using chemical hydrograph separation and antecedent stream base flow, which was assumed to reflect antecedent storage (Table 4). The relationship between pre-event water proportion and subsurface storage for the base-case hillslope numerical experiment is depicted in Figure 11. Just as a hysteretic relationship was found between storage and streamflow in the hillslope model (Figure 6), a hysteretic counterclockwise relationship was observed between subsurface storage and pre-event water proportion. Before the rain event began, and long after the rain event ended, the relationship between storage and pre-event water proportion had a positive slope, as less storage over time led to falling chloride values. During and directly after the rain event, the slope between storage and pre-event water proportion was negative, meaning that greater storage led to lower chloride values with the influx of low chloride rain.

4. Discussion

4.1. What Controls Pre-event Water Proportion of Stormflow in Urbanizing Areas?

Both methods used to address Question 1 indicate that rainfall depth plays a primary role in controlling pre-event water proportion within a single watershed. Of the factors investigated (rainfall depth, rainfall duration, time since last rain, base flow before storm, and watershed size), rainfall depth had the closest relationship to pre-event water proportion in Dead Run subwatersheds (Table 4 and Figure 5). Hillslope numerical experiments also demonstrated that variation in rainfall depth led to a greater change in pre-event water proportion compared to changes in initial storage conditions (represented by initial water table position). The "wetter" simulation, with a 25% increase in initial water table depth, was compared to simulations with rainfall depth changes of 25% ("smaller" and "larger" storm conditions of 0.75 and 1.25 cm rainfall, corresponding to a 25% decrease and increase from the base-case rainfall depth of 1 cm). Figure 4 shows that the pre-event water proportion resulting from a 25% change in rainfall depth was greater than that resulting from a 25% change in initial water table depth. Ranges in rainfall depth are commonly greater than 25%, and these larger variations are represented by the "smallest" and "largest" storms (0.25 and 2.5 cm; Table 3). As expected, this variability in rainfall depth led to an even greater change in pre-event water proportion compared to initial water table position.

The pre-event water proportion of total stormflow for the hillslope numerical experiments was greatest for the case of smallest rainfall (0.98), and was generally greater than 0.85 except for the impervious (0.14) and largest (0.74) storm cases (Table 3). Pre-event water proportions found using chemical hydrograph separation in Dead Run subwatersheds ranged from 0.14 to 0.94, which nearly matches the range of the simulated pre-event water proportion values (0.14–0.98). For the five numerical experiments with varying rainfall depths, pre-event water fraction was inversely proportional to rainfall depth (Figure 5). Over storms with the same range of rainfall depths (0.25–2.5 cm), pre-event water proportion values in Dead Run showed the same overall trend, but decreased more dramatically and was more nonlinear than those simulated.

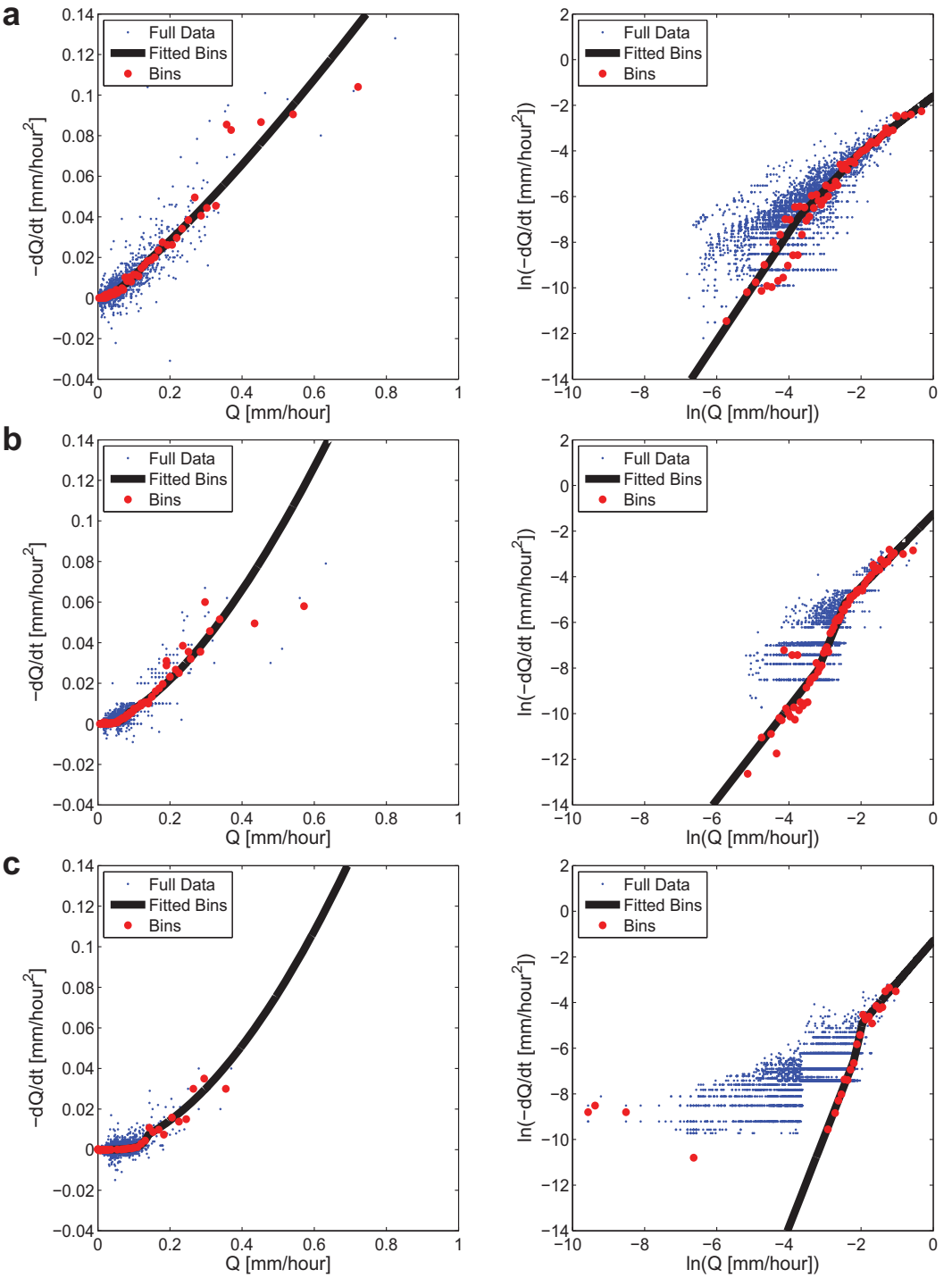

Figure 8. Natural logarithm of hourly change in streamflow as a function of natural logarithm of streamflow shown as (left) linear and (right) log scales for (a) Dead Run, (b) Delight, and (c) Baisman Run, along with bin means and bin fits.

We would not expect a direct correspondence between the two methods because the hillslope numerical experiments are not simulating the conditions in Dead Run. Some key differences are contributing area and drainage connection. Model simulations were conducted for a single hillslope, where the possible contributing area is limited, while by comparison the contributing area for stormflow in even a small subwatershed can vary dramatically and may be activated nonlinearly with rainfall depth. Also, the greater impervious surface coverage (at least 45%) and the direct connection between the land surface and streams in Dead Run

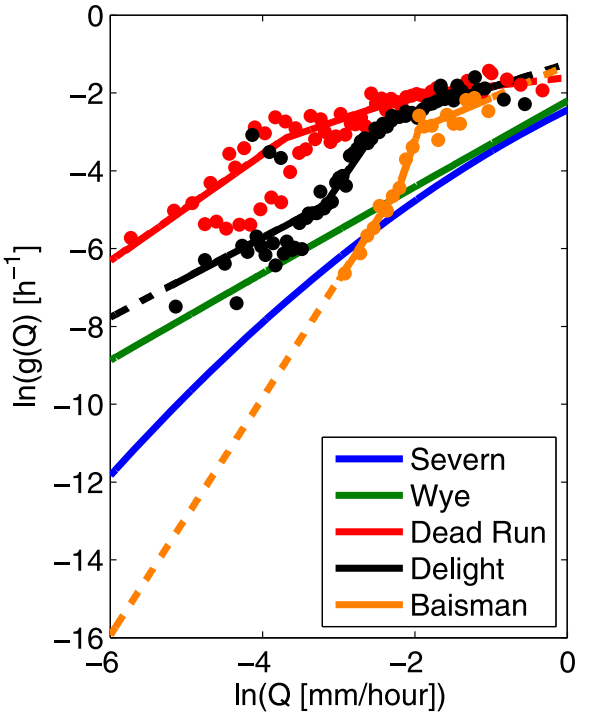

Figure 9. Natural logarithm of streamflow sensitivity as a function of natural logarithm of streamflow along with bins for three Baltimore, MD study watersheds and previously published work [*Kirchner*, 2009].

subwatersheds led to greater event water as compared to the hillslope numerical experiments. The hillslope numerical experiments also indicated that increased impervious surface area (represented by decreased hydraulic conductivity and porosity) led to a larger proportion of event water in streamflow. This was expected due to greater infiltration-excess overland flow directly carrying low-chloride rainwater to the stream.

4.2. What Controls the Relationship Between Subsurface Storage and Streamflow Along an Urban-to-Rural Gradient?

Watersheds with more urban development had greater streamflow sensitivity (Figure 9). The higher streamflow sensitivity in urban watersheds produced a feedback where increased storage due to precipitation events led to larger increases in streamflow as well as faster streamflow recession. The *Kirchner* [2009] methodology covers the entire range of streamflow and its relationship to storage. We can examine just storm events by using observations of stormflow and storage before storm events. Figure 12 shows stormflow versus precipitation at Dead Run at Franklintown, with size of markers indicating the magnitude of base flow. The magnitude of base flow, serving as a proxy for storage, did not have a discernible effect on stormflow response. Rainfall depth had a tight relationship with stormflow in Dead Run at Franklintown, as it was also found to be the primary control on pre-event water proportion in chemical hydrograph separation in this watershed and hillslope numerical experiments. Numerous previous studies have observed a threshold between precipitation and storm response or between storage and storm response [*Evett and Dutt*, 1985; *Sidle et al*., 2000; *Li and Gong*, 2002; *Rezaur et al*., 2003; *Tromp-van Meerveld and McDonnell*, 2006; *Hood et al*., 2007; *Spence*, 2007; *Zehe et al*., 2007; *Detty and McGuire*, 2010; *Graham and McDonnell*, 2010; *McGuire and McDonnell*, 2010; *Seibert et al*., 2011]. In contrast, for this watershed such a threshold was not observed. Almost every storm event produced a storm response, although the relationship between precipitation and stormflow was nonlinear such that an increase in rainfall led to a greater increase in stormflow for larger storms.

The storage-streamflow relationship developed using the simple dynamical systems approach, which assumes a single relationship between storage and streamflow derived from falling limbs of hydrographs, did not capture the hysteretic behavior observed in the hillslope numerical experiments. As seen by comparing Figures 4a and 4c, subsurface storage responded to rainfall input on a much longer time scale than did streamflow. Streamflow returned to base flow levels while subsurface storage was still high. The hysteresis between streamflow and storage may be a combination of two factors, the fast response of saturation-excess overland flow to the stream and the slow and temporally variable groundwater contributions as a result of the formation of a groundwater mound near the stream. The hydraulic head in the shallow subsurface showed a groundwater mound that developed and dissipated as a response to the storm event (Figure 7). This groundwater mound led to an increase in hydraulic gradient near the stream in early storm response with increased groundwater contributions to the stream. Later, when the mound dissipated and the hydraulic gradient returned to a constant value along the hillslope, the decreased hydraulic gradient led to smaller groundwater contributions to the stream. Both dissipation of the groundwater mound and cessation of overland flow contribute to the phenomenon observed where streamflow returns to base flow values more quickly than overall hillslope subsurface storage, leading to hysteretic relationship. Previous

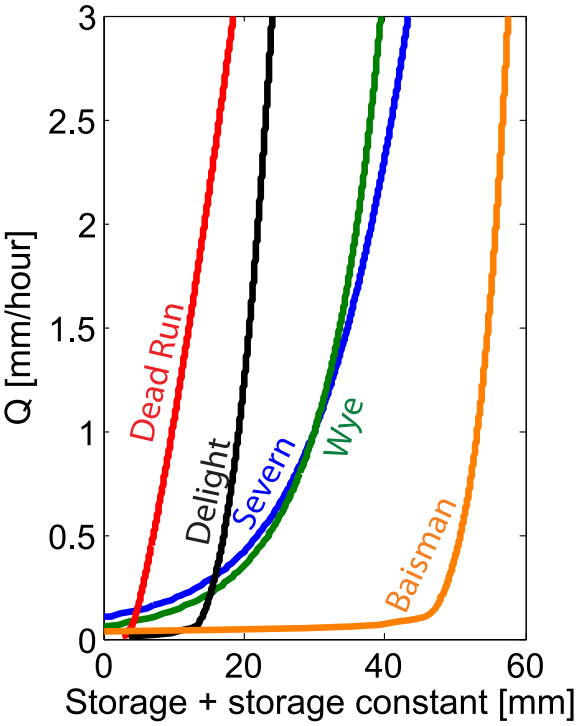

Figure 10. Streamflow as a function of storage using the simple dynamical systems analysis, where storage is determined by integration, and therefore includes an unknown constant of integration (equation (4)).

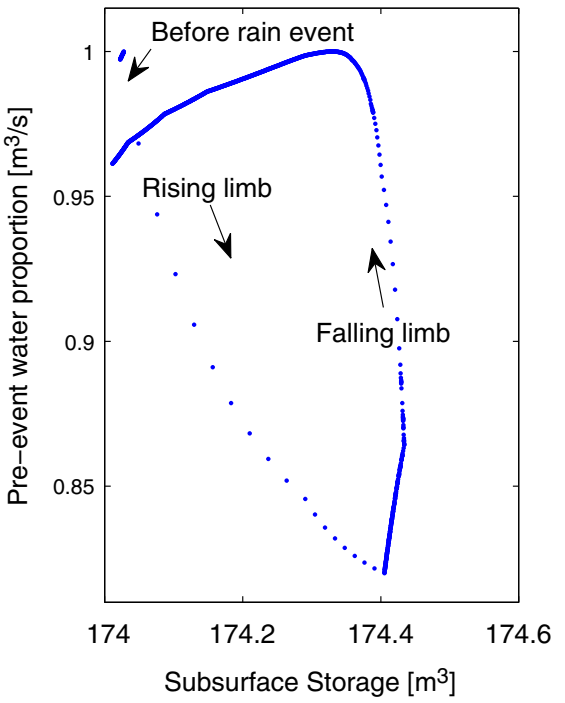

Figure 11. Pre-event water proportion as a function of subsurface storage using base-case parameters in hillslope numerical experiments. Arrows indicate time, where the terms "rising limb" and "falling limb" correspond to the components of the associated hydrograph for pre-event water proportion.

researchers have also observed a clockwise hysteretic relationship between storage and streamflow [*Kendall et al*., 1999; *Sayama et al*., 2011; *Xu et al*., 2012; *Weill et al*., 2013], where streamflow values during wetting are greater than those during drying for the same storage conditions. *Weill et al*. [2013] have suggested that the lower the initial saturation of the watershed, the greater the hysteresis in the relationship between storage and streamflow. This greater hysteresis under unsaturated conditions may result from the larger number of possible spatial configurations of subsurface storage, where each configuration may result in different streamflow values [*Weill et al*., 2013]. Investigators have called for a better understanding and representation of the hysteresis in the storage-streamflow relationship [*Beven*, 2006; *Spence*, 2010], but this hysteresis complicates the one-to-one simple dynamical systems approach by *Kirchner* [2009], as explored by *Xu et al*. [2012].

4.3. What Is the Relationship Between Pre-event Water Proportion of Stormflow and Subsurface Storage in Urban Areas?

Both chemical hydrograph separation in small, urban watersheds (Figure 5) and hillslope numerical experiments (Figure 4) indicate that prestorm storage conditions play a secondary role in determining pre-event water proportion in small, urban watersheds and in hillslope numerical experiments. The lack of a relation between storage (represented by prestorm base flow) and pre-event water proportion in chemical hydrograph separation was unanticipated because of previous work in which storage was found to play an important role in determining pre-event water proportion [*Burns et al*., 2001; *Pellerin et al*., 2008]. Instead, rainfall depth was the largest factor in determining pre-event water proportion in both hillslope numerical experiments and chemical hydrograph separation (as discussed in section 4.1).

There was a directional change in the relationship between storage and pre-event water proportion that was observed between recession and event periods (Figure 11). This is likely due to a number of

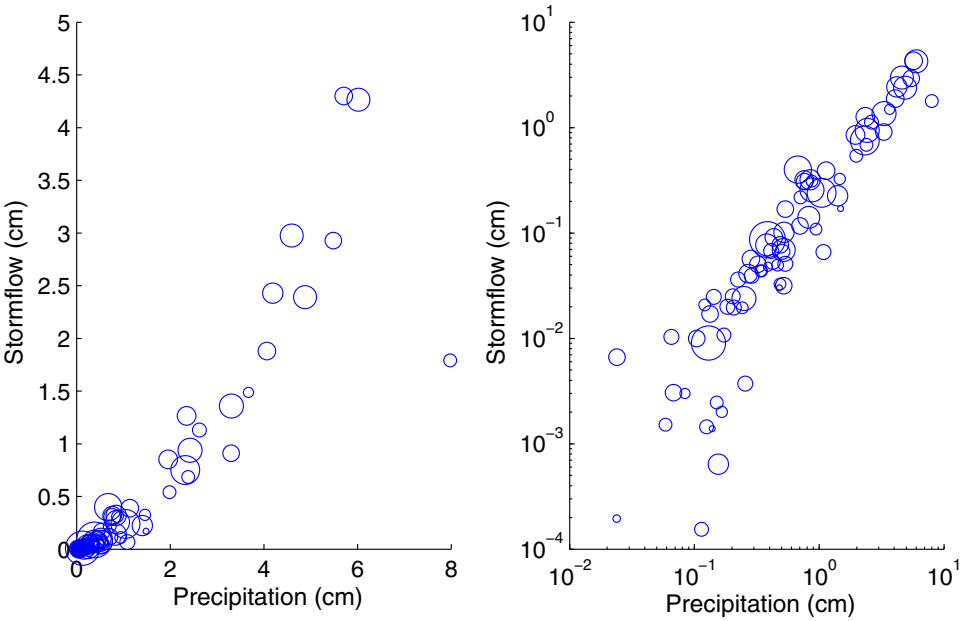

Figure 12. Precipitation depth versus stormflow during storm events in Dead Run at Franklintown (DRKR) on (left) linear and (right) log-log axes. Circle size is proportional to pre-event streamflow (base flow). Stormflow was calculated from USGS streamflow records using the straight-line method for hydrograph separation, while maintaining equal pre and poststorm base flow values. Precipitation values were averaged over the watershed from bias-corrected Hydro-NEXRAD radar rainfall values [*Smith et al*., 2012]. Only isolated storm events were used, such that a direct response between a specific precipitation event and storm response could be manually identified.

factors, such as the streamflow-storage relationship being hysteretic (Figure 6) and the concentration of chloride in groundwater not being constant during either base flow or the storm period. This can be seen during base flow (later times in Figure 4b), but is not clearly observable during the storm period because the chloride signal solely from groundwater is not visible. While this phenomenon may not be commonly observed in urban groundwater systems of a much larger scale, the hillslope model here was small enough that chloride in groundwater could become depleted. There was chloride entering the hillslope model from "regional flow" (up-gradient third-type transport boundary condition; Figure 1), but the chloride entering the system, even at the same concentration as the initial concentration (0.2 kg/m^3), did not completely replenish the chloride leaving through streamflow. This might be analogous to large urban aquifers over longer periods of time. For example, during periods when road salt is not being applied, chloride exits the subsurface through groundwater contributions to streamflow, but chloride is not being added to the system at the same rate. Therefore, the chloride mass in the overall reservoir decreases over time. This decrease in total mass is likely not observable in streamflow because the regional reservoir is large and is usually replenished every winter. Also, low-chloride rain that enters the system and remains relatively shallow may set up a concentration gradient where chloride concentration is related to flow path travel time. This gradient would not affect our chemical hydrograph separation during the storm period because the chloride concentration just before the rain event was used for the separation. Nonetheless, a nonconstant, pre-event tracer concentration complicates the chemical hydrograph separation method, as others have pointed out [*Gremillion et al*., 2000; *Kirchner*, 2003].

4.4. Limitations of Water Balance-Based Approach in an Urban Setting

As indicated in *Bhaskar and Welty* [2012], the water balances of Baltimore watersheds are considerably altered compared to their nearby rural counterparts. Watershed inflows and outflows, in particular, infiltration and inflow (I&I) of groundwater and storm water into wastewater pipes, play an important role in the Baltimore water balance. I&I and other aspects of the water balance related to urban infrastructure are not available at spatiotemporal scales similar to streamflow and precipitation. For example, monthly I&I data were provided to us by municipal governments, but I&I is commonly known to vary dramatically during storm events [*Belhadj et al*., 1995]. Therefore, the simple dynamical systems analysis for the study watersheds was carried out in the form presented by *Kirchner* [2009], in which the water balance (equation (2)) was composed of precipitation, evapotranspiration, and streamflow without additional urban water balance

components. The urban water balance terms that were neglected in equation (2), in particular I&I, may have affected the results that were generated using this method. If contributions of I&I were significant compared to streamflow, as was found in *Bhaskar and Welty* [2012] for two Baltimore City, MD streams, the recession (change in streamflow for a given change in storage) may have been interpreted to be faster than was actually the case due to the confounding factor of infiltration into wastewater pipes (or vice versa for exfiltration from wastewater pipes during storms). The effect of this omission may be similar to previously studied effects of anthropogenic factors on recession constants [*Wang and Cai*, 2010].

5. Summary and Implications

Our findings can be summarized as follows:

1. Chemical hydrograph separation for small, nested urban watersheds indicated that rainfall depth was the primary control on pre-event water proportion (Figure 5). The storage condition before the storm event appeared to play little role in affecting pre-event water proportion (Table 4) or streamflow response (Figure 12).
2. Hillslope numerical experiments also demonstrated that rainfall depth played a primary role in determining pre-event water proportion and streamflow response. Imperviousness contributed as well, reducing pre-event water proportion to a value of 0.02 at peak streamflow. Numerical experiments showed that the relationship between storage and streamflow (Figure 6) was clockwise hysteretic and the relationship between storage and pre-event water proportion (Figure 11) was counterclockwise hysteretic.
3. The simple dynamical systems analysis based on *Kirchner* [2009] showed that streamflow sensitivity was greater in watersheds characterized by a larger degree of urbanization (Figure 9). This meant that the change in streamflow for a given change in storage was larger for more urbanized watersheds.

We found that rainfall depth, not storage, was the primary control on pre-event water proportion, in contrast to previous studies that found storage to be important to determining pre-event water proportion [*Burns et al.*, 2001; *Pellerin et al.*, 2008]. The large proportion of pre-event water was particularly surprising for urban watersheds, in which the interaction between groundwater and surface water is commonly assumed to be more limited than in other settings with more permeable surface cover. The "fill-and-spill" streamflow generation mechanism [*Tromp-van Meerveld and McDonnell*, 2006], does not seem to apply well to the urban watersheds studied here. There was little if any threshold in the relationship between precipitation and stormflow in Dead Run (Figure 12). Furthermore, this hypothesized mechanism would imply that initial storage conditions (how filled storage reservoirs are before the rain event) would play a major role in either determining the threshold or the amount of stormflow generated for the same rainfall depth; this also did not seem to be the case here (Figure 12).

Pre-event water largely resides in the subsurface before a rain event. The contribution of pre-event water to stormflow and the maintenance of base flow demonstrate the interaction between subsurface and surface water during both stormflow and base flow. In watersheds with about 50% impervious surface cover, pre-event water can account for more than 50% of stormflow (Table 4). There are several possible explanations for how groundwater and surface water are observed to be interacting in these urban watersheds, where groundwater level (or subsurface storage) appears to play a secondary role in storm response. First, the storage reservoir in Dead Run may be small and therefore is almost always filled by any precipitation event, before spilling occurs. This does not mean that the watershed soils are always near saturation, but rather that the reservoir of storage that contributes to streamflow may be a small portion of the watershed. Second, the conditions studied here were relatively similar in terms of storage, whereas more variation in storage may have a larger effect on stormflow response. Third, there may be a discrepancy between the subsurface storage that our metrics are quantifying and the subsurface storage that is affecting stormflow response. Last, it is possible that the interactions between groundwater and surface water are important but are unaffected by changes in storage condition. There is some evidence for this last possibility based on the streamflow sensitivity function (Figure 9). Dead Run has the highest streamflow sensitivity of the watersheds studied, but that streamflow sensitivity is relatively constant over the range of observed streamflow. In comparison to the other watersheds, in Dead Run the streamflow response to an increase in storage due to precipitation is not affected much by the initial storage (or streamflow) conditions in the watershed. All of the possibilities listed here are opportunities for future research.

Acknowledgments
This work benefitted from use of bias-corrected Hydro-NEXRAD radar-rainfall fields provided by Mary Lynn Baeck and Jim Smith (Princeton University) and meteorological data from the McDonogh station provided by Gordon Heisler and Emma Noonan Powell (USFS). We are grateful for assistance in data processing by Joshua Cole, Roxanne Sanderson, Kelsey Weaver, and Phillip Larson and helpful discussions with Andrew J. Miller (UMBC CUERE). This manuscript benefitted from useful feedback from Dennis O'Carroll, Harihar Rajaram, and two anonymous reviewers. This research was supported by National Science Foundation (NSF) grants DGE-0549469, EF-0709659, CBET-0854307, CBET-1058038, and EAR-1349815 and NOAA grant NA10OAR431220. In addition, this work builds upon field and data infrastructure supported by the NSF Long-Term Ecological Research (LTER) Program (Baltimore Ecosystem Study) under NSF grants DEB-0423476 and DEB-1027188. The model simulations and specific conductance data are freely available from the authors. HydroNEXRAD precipitation data are available at http://oshydro.umbc.edu/GFhydroNEXRAD/.

References

Ajami, H., M. F. McCabe, J. P. Evans, and S. Stisen (2014), Assessing the impact of model spin-up on surface water-groundwater interactions using an integrated hydrologic model, *Water Resour. Res.*, *50*, 2636–2656, doi:10.1002/2013WR014258.

Allen, R. G., L. S. Pereira, D. Raes, and M. Smith (1998), Crop Evapotranspiration: Guidelines for Computing Crop Water Requirements, *FAO Irrig. Drain. Pap. 56*, Food and Agric. Organ. of the U. N., Rome.

Belhadj, N., C. Joannis, and G. Raimbault (1995), Modelling of rainfall induced infiltration into separate sewerage, *Water Sci. Technol.*, *32*(1), 161–168, doi:10.1016/0273-1223(95)00551-W.

Beven, K. (2006), Searching for the Holy Grail of scientific hydrology: $Q_t = (S,R, \Delta t)$ A as closure, *Hydrol. Earth Syst. Sci.*, *10*(5), 609–618.

Bhaskar, A. S., and C. Welty (2012), Water balances along an urban-to-rural gradient of metropolitan Baltimore, 2001–2009, *Environ. Eng. Geosci.*, *18*(1), 37–50, doi:10.2113/gseegeosci.18.1.37.

Burns, D. A. (2002), Stormflow-hydrograph separation based on isotopes: The thrill is gone—What's next?, *Hydrol. Processes*, *16*(7), 1515–1517, doi:10.1002/hyp.5008.

Burns, D. A., J. J. McDonnell, R. P. Hooper, N. E. Peters, J. E. Freer, C. Kendall, and K. Beven (2001), Quantifying contributions to storm runoff through end-member mixing analysis and hydrologic measurements at the Panola Mountain Research Watershed (Georgia, USA), *Hydrol. Processes*, *15*(10), 1903–1924, doi:10.1002/hyp.246.

Buttle, J. M. (1994), Isotope hydrograph separations and rapid delivery of pre-event water from drainage basins, *Prog. Phys. Geogr.*, *18*(1), 16–41, doi:10.1177/030913339401800102.

Buttle, J. M., A. M. Vonk, and C. H. Taylor (1995), Applicability of isotopic hydrograph separation in a suburban basin during snowmelt, *Hydrol. Processes*, *9*(2), 197–211, doi:10.1002/hyp.3360090206.

Detty, J. M., and K. J. McGuire (2010), Threshold changes in storm runoff generation at a till-mantled headwater catchment, *Water Resour. Res.*, *46*, W07525, doi:10.1029/2009WR008102.

Ehsanzadeh, E., C. Spence, G. van der Kamp, and B. McConkey (2012), On the behaviour of dynamic contributing areas and flood frequency curves in North American Prairie watersheds, *J. Hydrol.*, *414–415*, 364–373, doi:10.1016/j.jhydrol.2011.11.007.

Evett, S. R., and G. R. Dutt (1985), Effect of slope and rainfall intensity on erosion from sodium dispersed, compacted earth microcatchments 1, *Soil Sci. Soc. Am. J.*, *49*(1), 202–206, doi:10.2136/sssaj1985.03615995004900010040x.

Freeze, R. A. (1974), Streamflow generation, *Rev. Geophys.*, *12*(4), 627–647, doi:10.1029/RG012i004p00627.

Gelhar, L. W., and J. L. Wilson (1974), Ground-water quality modeling, *Ground Water*, *12*(6), 399–408, doi:10.1111/j.1745-6584.1974.tb03050.x.

Genereux, D. P., and R. P. Hooper (1999), Oxygen and hydrogen isotopes in rainfall-runoff studies, in *Isotope Tracers in Catchment Hydrology*, edited by C. Kendall and J. J. McDonnell, Elsevier Sci., pp. 319–346, Elsevier, Amsterdam, Netherlands.

Graham, C. B., and J. J. McDonnell (2010), Hillslope threshold response to rainfall: 2. Development and use of a macroscale model, *J. Hydrol.*, *393*, 77–93, doi:10.1016/j.jhydrol.2010.03.008.

Gremillion, P., A. Gonyeau, and M. Wanielista (2000), Application of alternative hydrograph separation models to detect changes in flow paths in a watershed undergoing urban development, *Hydrol. Processes*, *14*(8), 1485–1501, doi:10.1002/1099-1085(20000615)14:8<1485::AID-HYP988>3.0.CO;2-1.

Hood, M. J., J. C. Clausen, and G. S. Warner (2007), Comparison of stormwater lag times for low impact and traditional residential development, *J. Am. Water Resour. Assoc.*, *43*(4), 1036–1046, doi:10.1111/j.1752-1688.2007.00085.x.

Hopp, L., and J. J. McDonnell (2009), Connectivity at the hillslope scale: Identifying interactions between storm size, bedrock permeability, slope angle and soil depth, *J. Hydrol.*, *376*(3–4), 378–391.

James, A. L., J. J. McDonnell, I. Tromp-van Meerveld, and N. E. Peters (2010), Gypsies in the palace: Experimentalist's view on the use of 3-D physics-based simulation of hillslope hydrological response, *Hydrol. Processes*, *24*(26), 3878–3893, doi:10.1002/hyp.7819.

Jones, J. P., E. A. Sudicky, A. E. Brookfield, and Y.-J. Park (2006), An assessment of the tracer-based approach to quantifying groundwater contributions to streamflow, *Water Resour. Res.*, *42*, W02407, doi:10.1029/2005WR004130.

Kaushal, S. S., and K. T. Belt (2012), The urban watershed continuum: Evolving spatial and temporal dimensions, *Urban Ecosyst.*, *15*(2), 409–435, doi:10.1007/s11252-012-0226-7.

Kendall, C., and J. J. McDonnell (1999), Isotope Tracers in Catchment Hydrology (Developments in Water Science), Elsevier Sci., Amsterdam, Netherlands.

Kendall, K. A., J. B. Shanley, and J. J. McDonnell (1999), A hydrometric and geochemical approach to test the transmissivity feedback hypothesis during snowmelt, *J. Hydrol.*, *219*(3-4), 188–205, doi:10.1016/S0022-1694(99)00059-1.

Kienzler, P. M., and F. Naef (2008), Subsurface storm flow formation at different hillslopes and implications for the "old water paradox," *Hydrol. Processes*, *22*(1), 104–116, doi:10.1002/hyp.6687.

Kirchner, J. W. (2003), A double paradox in catchment hydrology and geochemistry, *Hydrol. Processes*, *17*(4), 871–874, doi:10.1002/hyp.5108.

Kirchner, J. W. (2009), Catchments as simple dynamical systems: Catchment characterization, rainfall-runoff modeling, and doing hydrology backward, *Water Resour. Res.*, *45*, W02429, doi:10.1029/2008WR006912.

Krier, R., P. Matgen, K. Goergen, L. Pfister, L. Hoffmann, J. W. Kirchner, S. Uhlenbrook, and H. H. G. Savenije (2012), Inferring catchment precipitation by doing hydrology backward: A test in 24 small and mesoscale catchments in Luxembourg, *Water Resour. Res.*, *48*, W10525, doi:10.1029/2011WR010657.

Li, X.-Y., and J.-D. Gong (2002), Compacted microcatchments with local earth materials for rainwater harvesting in the semiarid region of China, *J. Hydrol.*, *257*(1–4), 134–144, doi:10.1016/S0022-1694(01)00550-9.

Liu, L., and T. Guo (2003), Determining the condition of hot mix Asphalt specimens in dry, water-saturated, and frozen conditions using GPR, *J. Environ. Eng. Geophys.*, *8*(2), 135–142, doi:10.4133/JEEG8.2.143.

Majone, B., A. Bertagnoli, and A. Bellin (2010), A non-linear runoff generation model in small Alpine catchments, *J. Hydrol.*, *385*(1–4), 300–312, doi:10.1016/j.jhydrol.2010.02.033.

McDonnell, J. J. (2003), Where does water go when it rains? Moving beyond the variable source area concept of rainfall-runoff response, *Hydrol. Processes*, *17*, 1869–1875, doi:10.1002/hyp.5132.

McDonnell, J. J., and R. Woods (2004), On the need for catchment classification, *J. Hydrol.*, *299*(1-2), 2–3, doi:10.1016/j.jhydrol.2004.09.003.

McGuire, K. J., and J. J. McDonnell (2010), Hydrological connectivity of hillslopes and streams: Characteristic time scales and nonlinearities, *Water Resour. Res.*, *46*, W10543, doi:10.1029/2010WR009341.

McNamara, J. P., D. Tetzlaff, K. Bishop, C. Soulsby, M. Seyfried, N. E. Peters, B. T. Aulenbach, and R. Hooper (2011), Storage as a metric of catchment comparison, *Hydrol. Processes*, *25*, 3364–3371, doi:10.1002/hyp.8113.

Meriano, M., K. W. F. Howard, and N. Eyles (2011), The role of midsummer urban aquifer recharge in stormflow generation using isotopic and chemical hydrograph separation techniques, *J. Hydrol.*, *396*(1-2), 82–93, doi:10.1016/j.jhydrol.2010.10.041.

Nolan, K. M., and B. R. Hill (1990), Storm-runoff generation in the Permanente Creek drainage basin, west central California—An example of flood-wave effects on runoff composition, *J. Hydrol.*, *113*(1-4), 343–367, doi:10.1016/0022-1694(90)90183-X.
Oswald, C. J., M. C. Richardson, and B. A. Branfireun (2011), Water storage dynamics and runoff response of a boreal Shield headwater catchment, *Hydrol. Processes*, *25*, 3042–3060, doi:10.1002/hyp.8036.
Park, Y.-J., E. A. Sudicky, A. E. Brookfield, and J. P. Jones (2011), Hydrologic response of catchments to precipitation: Quantification of mechanical carriers and origins of water, *Water Resour. Res.*, *47*, W12515, doi:10.1029/2010WR010075.
Paul, M. J., and J. L. Meyer (2001), Streams in the urban landscape, *Annu. Rev. Ecol. Syst.*, *32*(1), 333–365, doi:10.1146/annurev.ecolsys.32.081501.114040.
Pellerin, B. A., W. M. Wollheim, X. Feng, and C. J. Vörösmarty (2008), The application of electrical conductivity as a tracer for hydrograph separation in urban catchments, *Hydrol. Processes*, *22*(12), 1810–1818, doi:10.1002/hyp.6786.
Rezaur, R., H. Rahardjo, E. Leong, and T. Lee (2003), Hydrologic behavior of residual soil slopes in Singapore, *J. Hydrol. Eng.*, *8*(3), 133–144, doi:10.1061/(ASCE)1084-0699(2003)8:3(133).
Rose, S., and N. E. Peters (2001), Effects of urbanization on streamflow in the Atlanta area (Georgia, USA): A comparative hydrological approach, *Hydrol. Processes*, *15*(8), 1441–1457, doi:10.1002/hyp.218.
Sayama, T., J. J. McDonnell, A. Dhakal, and K. Sullivan (2011), How much water can a watershed store?, *Hydrol. Processes*, *25*, 3899–3908, doi:10.1002/hyp.8288.
Seibert, J., K. Bishop, L. Nyberg, and A. Rodhe (2011), Water storage in a till catchment. I: Distributed modelling and relationship to runoff, *Hydrol. Processes*, *25*(25), 3937–3949, doi:10.1002/hyp.8309.
Sidle, R. C., Y. Tsuboyama, S. Noguchi, I. Hosoda, M. Fujieda, and T. Shimizu (2000), Stormflow generation in steep forested headwaters: A linked hydrogeomorphic paradigm, *Hydrol. Processes*, *14*, 369–385, doi:10.1002/(SICI)1099-1085(20000228)14:3<369::AID-HYP943>3.0.CO;2-P.
Sidle, W. C., and P. Y. Lee (1999), Urban stormwater tracing with the naturally occurring deuterium isotope, *Water Environ. Res.*, *71*, 1251–1256, doi:10.2175/106143096X122357.
Sklash, M. G., and R. N. Farvolden (1979), The role of groundwater in storm runoff, *J. Hydrol.*, *43*(1-4), 45–65, doi:10.1016/0022-1694(79)90164-1.
Smith, J. A., M. L. Baeck, G. Villarini, C. Welty, A. J. Miller, and W. F. Krajewski (2012), Analyses of a long-term, high-resolution radar rainfall data set for the Baltimore metropolitan region, *Water Resour. Res.*, *48*, W04504, doi:10.1029/2011WR010641.
Spence, C. (2007), On the relation between dynamic storage and runoff: A discussion on thresholds, efficiency, and function, *Water Resour. Res.*, *43*, W12416, doi:10.1029/2006WR005645.
Spence, C. (2010), A paradigm shift in hydrology: Storage thresholds across scales influence catchment runoff generation, *Geogr. Compass*, *4*, 819–833, doi:10.1111/j.1749-8198.2010.00341.x.
Spence, C., and M. Woo (2003), Hydrology of subarctic Canadian shield: Soil-filled valleys, *J. Hydrol.*, *279*(1–4), 151–166, doi:10.1016/S0022-1694(03)00175-6.
Teuling, A., I. Lehner, J. Kirchner, and S. Seneviratne (2010), Catchments as simple dynamical systems: Experience from a Swiss prealpine catchment, *Water Resour. Res.*, *46*, W10502, doi:10.1029/2009WR008777.
Therrien, R., R. G. McLaren, E. A. Sudicky, and S. M. Panday (2010), *HydroGeoSphere A Three-dimensional Numerical Model Describing Fully-integrated Subsurface and Surface Flow and Solute Transport*, Groundwater Simul. Group, Univ. of Waterloo, Waterloo, Ont., Canada.
Tromp-van Meerveld, H. J., and J. J. McDonnell (2006), Threshold relations in subsurface stormflow: 2. The fill and spill hypothesis, *Water Resour. Res.*, *42*, W02411, doi:10.1029/2004WR003800.
Tromp-van Meerveld, I., and M. Weiler (2008), Hillslope dynamics modeled with increasing complexity, *J. Hydrol.*, *361*, 24–40, doi:10.1016/j.jhydrol.2008.07.019.
United Nations (2014), World Urbanization Prospects: The 2014 Revision, Highlights (ST/ESA/SER.A/352), Department of Economic and Social Affairs, Population Division, United Nations, N. Y.
VerHoef, J., C. Welty, J. Miller, M. Grese, M. P. McGuire, R. Sanderson, S. Kaushal, and A. J. Miller (2011), *Preliminary Assessment of Real-Time Sensor Deployment in Baltimore Urban Watersheds*, *CUERE Tech. Rep. 2011/001*, Cent. for Urban Environ. Res. and Educ., UMBC, Baltimore, Md.
VerHoef, J. R. (2012), Spectral analysis of weekly and high-frequency stream chemistry data in urban watersheds, Master's thesis, Univ. of Maryland, Baltimore, Md.
Wagener, T., M. Sivapalan, P. Troch, and R. Woods (2007), Catchment classification and hydrologic similarity, *Geogr. Compass*, *1*, 901–931, doi:10.1111/j.1749-8198.2007.00039.x.
Wagener, T., M. Sivapalan, P. A. Troch, B. L. McGlynn, C. J. Harman, H. V. Gupta, P. Kumar, P. S. C. Rao, N. B. Basu, and J. S. Wilson (2010), The future of hydrology: An evolving science for a changing world, *Water Resour. Res.*, *46*, W05301, doi:10.1029/2009WR008906.
Walsh, C. J., A. H. Roy, J. W. Feminella, P. D. Cottingham, P. M. Groffman, and R. P. Morgan II (2005), The urban stream syndrome: Current knowledge and the search for a cure, *J. North Am. Benthol. Soc.*, *24*(3), 706–723.
Wang, D., and X. Cai (2010), Comparative study of climate and human impacts on seasonal baseflow in urban and agricultural watersheds, *Geophys. Res. Lett.*, *37*, L06406, doi:10.1029/2009GL041879.
Weiler, M., and J. McDonnell (2004), Virtual experiments: A new approach for improving process conceptualization in hillslope hydrology, *J. Hydrol.*, *285*(1-4), 3–18.
Weill, S., M. Altissimo, G. Cassiani, R. Deiana, M. Marani, and M. Putti (2013), Saturated area dynamics and streamflow generation from coupled surface–subsurface simulations and field observations, *Adv. Water Resour.*, *59*, 196–208, doi:10.1016/j.advwatres.2013.06.007.
Wiles, T. J., and J. M. Sharp (2008), The secondary permeability of impervious cover, *Environ. Eng. Geosci.*, *14*(4), 251–265, doi:10.2113/gseegeosci.14.4.251.
Xu, N., J. E. Saiers, H. F. Wilson, and P. A. Raymond (2012), Simulating streamflow and dissolved organic matter export from a forested watershed, *Water Resour. Res.*, *48*, W05519, doi:10.1029/2011WR011423.
Zehe, E., and M. Sivapalan (2009), Threshold behaviour in hydrological systems as (human) geo-ecosystems: Manifestations, controls, implications, *Hydrol. Earth Syst. Sci.*, *13*(7), 1273–1297, doi:10.5194/hess-13-1273-2009.
Zehe, E., H. Elsenbeer, F. Lindenmaier, K. Schulz, and G. Blöschl (2007), Patterns of predictability in hydrological threshold systems, *Water Resour. Res.*, *43*, W07434, doi:10.1029/2006WR005589.